Using Footsteps to Estimate Changes in the Desired Gait Speed of an Exoskeleton User

Roopak M. Karulkar[1], Patrick M. Wensing[1]

***Abstract*—This letter outlines an estimation framework to detect changes in the intended gait speed of an assistive exoskeleton user during walking. A twice-per-step estimation strategy, termed a Buttressed Kalman Filter, is presented to leverage changes in foot placement to infer changes in desired speed. The first stage of the estimator applies a Bayesian update to the center of mass state at midstance before it is passed to a Kalman filter in the second stage. The Bayesian update relies on the comparison between a predicted step length computed as a function of the intended velocity and the measured step length, the difference of which provides insight into user intent. This framework was tested with sensor data acquired from walking trials in an Ekso GT exoskeleton for users with and without incomplete Spinal Cord Injuries (iSCIs) from the middle to lower spine. The trials consisted of users changing their gait speed upon command. The presented framework was able to anticipate these desired changes before users physically changed their speed. It was also found that using measurements of the root mean square (RMS) current of the hip motors increased the effectiveness of the estimator in predicting intent changes for individuals with iSCIs.**

***Index Terms*—Exoskeletons, Intent Recognition, Physical Human-Robot Interaction**

I. Introduction

A. Motivation and Previous Work

EACH year there are 12,000 new spinal cord injury (SCI) cases in the US, in addition to the quarter of a million existing ones [1]. Traditionally, gait rehabilitation following SCI involves physiotherapists manually moving the affected person's legs through prescribed trajectories toward establishing new neural pathways to relearn walking. However, this process requires multiple physiotherapists per treatment session making it labor intensive and expensive. Additionally, since patients' legs are moved manually, the physiotherapists may suffer from exhaustion and may be unable to track the prescribed trajectories accurately.

Robotic exoskeletons, such as the Ekso GT [2], ReWalk Personal System [3], and Indego [4], have been cleared by the FDA for use as tools for gait rehabilitation due to their ability to repeatedly and accurately track the desired joint trajectories necessary for gait rehabilitation. This increased repeatability and accuracy may accelerate rehabilitation [5]. The use of exoskeletons also reduces the number of therapists per patient and the amount of work required from them. Exoskeleton usage has the potential to increase the patient's level of autonomy, and this increased level of autonomy requires fluent Human-Robot Interaction (HRI) in order to maintain safety and efficacy.

Fluency in HRI depends heavily on the ease with which the user can convey their intent to the robot to accomplish their desired goal. One indication of high fluency in HRI is the robot's ability to provide timely assistance to the user [6], and accurate assistance timing requires the robot to anticipate the user's actions [7]. Therefore, accurate intent detection is a key requirement in achieving the necessary fluency. Currently available exoskeletons rely on buttons and joysticks for the user to explicitly convey their intent. However, the goal of this work is to present an anticipative framework that detects intent changes more intuitively and without added interfaces.

Intent detection can be performed in multiple ways by leveraging HRI. A straightforward approach is to infer intent by comparing measurements of user activity to a discrete set of predefined actions stored in a database [8]. However, since generating comprehensive activity databases may be prohibitive, another approach is to treat intent as a continuous variable. Corteville et al. [9] studied point-to-point reaching movements and assumed the human to be in control of the point of interaction between the human and robot. They used the onboard position sensors to fit the user's motion to a bell-shaped velocity profile to predict the desired speed of the reaching motion. Similarly, user intent can be inferred by comparing the user's force contribution to the desired motion [10]. Alternatively, intent can be inferred based on how the user makes the robot interact with the environment. For example, in Brescanini et al. [11], Inertial Measurement Units (IMUs) were mounted to crutches to estimate their orientation. The estimated placement of crutch tips was then used to infer user intent variables such as stride length, direction, and stair ascent/descent.

To pose intent as a continuous variable in an estimator, intent evolution needs to first be characterized; this can be achieved using model-based or learning-based strategies. Model-based strategies use the dynamics of physics-based models and sensor feedback to infer user intent. Previous work on model-based user intention detection used Ground Reaction Force (GRF) patterns observed during walking to assist individuals with paraplegia while walking using a lower-extremity exoskeleton [12]. Work has also been done to infer intent using simplified models of locomotion called template models. These models can approximate key features of human gait using parameters such as leg length and weight, and can

Manuscript received: February, 24, 2021; Revised May, 24, 2021; Accepted June, 20, 2021.

This paper was recommended for publication by Editor Pietro Valdastri upon evaluation of the Associate Editor and Reviewers' comments. This work was supported by the National Science Foundation under Grant IIS-1734532

[1]Authors are with the Department of Aerospace and Mechanical Engineering, University of Notre Dame, Notre Dame, IN, USA. rkarulka@nd.edu

Digital Object Identifier (DOI): see top of this page.

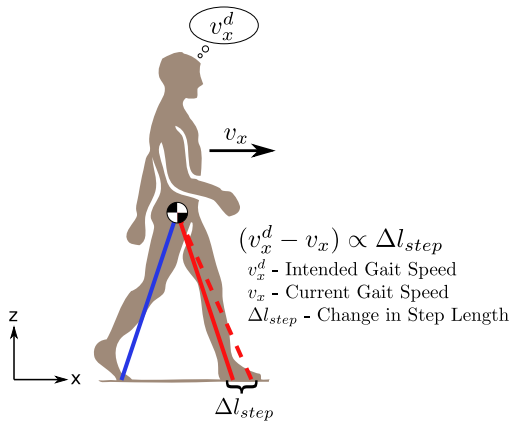

Fig. 1. Change in intended velocity may be inferred from change in step length

therefore be adapted to accommodate a wider range of users with varying physiology.

One example of a template model is the Bipedal Spring-Loaded Inverted Pendulum (B-SLIP) model [13], [14] that exhibits center of mass (CoM) trajectories similar to those of a person running or walking. This model exhibits hybrid dynamics to describe the various phases of human gait. As part of previous work, we developed a framework that used Interacting Multi-Model (IMM) estimation to infer an exoskeleton user's gait phase and velocity by comparing predicted B-SLIP CoM trajectories to sensor measurements [15]. However, the average gait speed for people with an SCI ranges from 0.2 m/s - 0.6 m/s [16] and it is difficult to find B-SLIP gaits at these velocities due to low passive stability [17]. Additionally, the inter- and intra-subject gait variability seen in human walking is increased due to spasticity following SCI, which increases the difficulty of intent estimation with these and other approaches.

In contrast to model-based strategies, learning-based strategies use gait data to form relationships between the observed gait and sensor measurements. Lee et al. used a Convolutional Neural Network (CNN) to predictively estimate user intent in real time with low error rates [18]. The CNN, which was trained using walking data from healthy individuals, uses measurements from various sensors such as electromyography (EMG), IMUs, and electrogoniometers to classify intent between level walking, ramp and stair ascent/descent. Gait patterns in individuals with iSCIs are dependent on the severity of their injury and the interaction with the robot. Therefore, data-driven approaches may require a large amount of training data to accommodate all the variability.

Since learning-based methods may require prohibitive amounts of data to achieve acceptable accuracy, this also makes it difficult to design controllers and estimators that accommodate multiple users. The scarcity of available training data may require the use of methods that have low data reliance. Thatte et al. developed an estimator that uses a Gaussian Process (GP) based Extended Kalman Filter [19] to estimate the user's gait phase during stance to control a prosthetic leg. GPs are one class of models that are well suited for use in data-scarce applications. Needing fewer training datasets may also allow designers to train for a wider variety of use scenarios such as varied assistive devices, terrains, and injury levels.

Learning-based strategies can be used to capture characteristics of gait that are difficult to model such as step-to-step variability, the presence of ambulatory devices, and the coupled dynamics of the human and the robot. The hybrid nature of legged locomotion dynamics alone increases the difficulty of control and state estimation for lower-limb assistive devices. Kalinowska et al. used a data-driven approximation of the SLIP dynamics to identify gait phases such as stance or swing, and events such as heel strike or toe-off [20]. Other methods that use the sensors onboard the exoskeleton have shown how intent may be inferred. Gambon et al. presented an algorithm [21] to identify instances where an exoskeleton user wanted to walk faster or slower than their nominal speed based on the Mahalanobis distance of the sensor measurements from the nominal trajectory.

The work presented in this letter outlines a method of intent recognition that relies on a simple model to exploit the relationship between velocity change and step length change, as illustrated in Fig. 1, to infer the intended gait speed of an exoskeleton user. Estimating the gait speed of an individual may increase the possibility for finer control of the gait and also limit the need to train for multiple discrete scenarios.

B. Contribution

Anticipative intent detection is a crucial requirement for the robot to fluently interact with and assist the user. The main contribution of this work is a new Bayesian estimation framework that relies on a simple model to anticipate a user's intent to change speeds before it happens physically. Since ground contacts greatly influence the stability of legged locomotion, it is hypothesized that user intent will be reflected in the contacts chosen. As such, the work presented in this letter explores exploiting changes in foot placement to infer the intended gait speed changes of an exoskeleton user.

The footstep model emulates the trends in footstep versus velocity in uninjured individuals as an indicator of intent change. An additional model for RMS hip motor currents was used for individuals with iSCIs to capture the users' interaction with the exoskeleton and improve estimation accuracy. This framework was evaluated on an experimental dataset containing speed change trials of subjects with and without iSCIs walking in an Ekso GT lower-limb exoskeleton. The framework is able to estimate whether the user wants to speed up or slow down, and does so before the user physically changes speed.

C. Overview

The remainder of the paper is organized as follows. Section II details the two-stage estimation framework used to incorporate information gained from foot placement into the intent estimation problem. The performance of this framework was evaluated on experimental data of exoskeleton walking trials and is discussed in Section III. Concluding remarks and future work are outlined in Section IV.

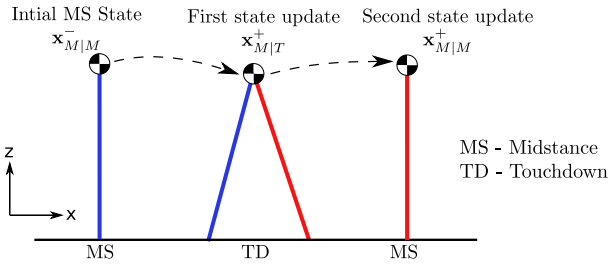

Fig. 2. Gait events in a step and estimation points

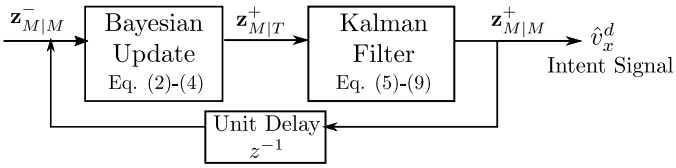

Fig. 3. Twice-per-step strategy to estimate user intent

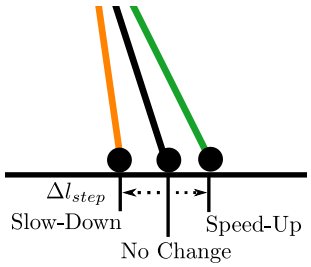

Fig. 4. The effect of velocity change on step length. Speed-up and slow-down increase and decrease the step length respectively.

II. Intent Detection

A. Estimation Framework

Legged locomotion is governed by ground contact, which suggests that features regarding contact will carry a great deal of information regarding user intent. Modulating foot placement while walking is an effective control mechanism to maintain stability [22] and step-to-step gait variability may be stabilizing responses to internal muscle noise [23]. Therefore, it has been shown that velocity changes at midstance (MS) influence foot placement at touchdown (TD) [24].

In order to detect user intent, it must first be quantified. Quantification of intent is a design choice, and given that the primary objective of the lower-extremity exoskeletons herein is gait rehabilitation, the intended gait velocity was deemed an appropriate quantity to represent intent. The state of the exoskeleton is represented in a vector

$$\mathbf{x} = [\mathbf{p}_{CoM}^{\top}, \mathbf{v}_{CoM}^{\top}]^{\top}$$

that contains the position and velocity of the exoskeleton user's CoM relative to the stance foot, reported with the units m and m/s respectively. To capture intent, the state was extended to include the desired gait velocity v_x^d in an augmented state vector $\mathbf{z} = [\mathbf{x}^{\top}, v_x^d]^{\top}$. The gait velocity v_x^d only represents the velocity in the sagittal plane. Velocity in the transverse plane (e.g., while turning) is neglected, as the exoskeleton restricts adduction/abduction of the legs. Overall, the state augmentation approach allows using estimation tools such as the Kalman filter directly on the intent.

It was assumed that intent changes made at the first MS are reflected in the placement of the foot at TD and then maintained as constant until the subsequent MS. As illustrated in Fig. 2, a step starts at MS, the footstep is finalized at TD, and the step is completed at the next MS. Therefore, a twice-per-step estimation strategy was used to estimate intent at TD and MS as shown in Fig. 3, where the unit delay represents the passing of estimates as initial conditions for the next estimation cycle.

There is a correlation between step length and walking velocity that can be exploited to infer changes in intended gait speed. People walking at lower velocities exhibit shorter step lengths, and an increase in velocity results in an increase in step length [17], as illustrated in Fig. 4. Such a velocity-step-length relationship can also be viewed as valid assuming that the walk ratio is roughly constant [25].

The walk ratio, defined as the ratio of the step length to cadence, is fairly invariant with respect to gait speeds for community ambulation, i.e., gait velocities greater than 0.8 m/s, despite age and terrain. It is affected when attention is divided between motor and cognitive tasks i.e., dual-task walking [26]. The walk ratio increases as speed decreases below community ambulation velocities [27] and is dependent on the nature and severity of injuries [28] during unassisted walking. In rehabilitation, the variability in the walk ratio may be reduced due to the stability provided by the exoskeleton structure and consistent timing of the exoskeleton assistance [29]. While the effects of exoskeleton-assisted walking on the walk ratio remain open, this analysis suggests that it is reasonable to assume a constant walk ratio for the work herein.

Since intent changes were primarily hypothesized to be inferred using the step length change information, a staged estimation scheme was considered that updates the intent state at the MS prior to the touchdown of the leading foot and then corrects the other state estimates at the terminal MS. A simple data-driven model of step length was used as a function of the velocity v_x at the MS prior to TD, desired velocity v_x^d, and leg length l_{leg}:

$$l_{step} = [v_x \ (v_x^d - v_x) \ l_{leg}]\boldsymbol{\kappa}, \tag{1}$$

where $\boldsymbol{\kappa}$ is a vector containing regression coefficients and the model output is a scalar value in meters. This model takes into consideration the nominal step length as a function of leg length, the current velocity, and desired velocity.

The step length model may be used as a measurement model in a Kalman filter framework to relate the intended gait speed to the measured step length. The estimator operates on the the state $\hat{\mathbf{z}}$ and its covariance $\mathbf{P}$. In the following equations, the superscripts $-$ and $+$ denote pre-/post-update states respectively, the subscripts M and T denote MS and TD respectively, and the bar denotes the update location. For instance, $\hat{\mathbf{z}}_{M|T}^{+}$ represents the state of the CoM at MS updated at TD.

Since the footstep model is data-driven and may have inaccuracies, a process noise covariance $\mathbf{Q}_T$ was added to

the state estimate covariance $\mathbf{P}^-_{M|M}$. Additionally, the estimated measurement covariance $\mathbf{\Sigma}_{yy}$ was computed using the Jacobian of the measurement model $\mathbf{H}_T$ and measurement covariance $\mathbf{R}_T$. The predicted step length from Eq. (1) was compared to the measured step length $\tilde{\mathbf{y}}_T$. The state at MS $\hat{\mathbf{z}}^-_{M|M}$ and its covariance were then updated using a Bayesian update as shown in Eq. (3) and Eq. (4).

$$\begin{aligned}
\hat{\mathbf{y}}_T &= l_{step}(\hat{v}_x, \hat{v}^d_x, l_{leg}) \\
\mathbf{H}_T &= \left.\frac{\partial \hat{\mathbf{y}}_T}{\partial \mathbf{z}}\right|_{\hat{\mathbf{z}}} \\
\mathbf{\Sigma}_{yy} &= \mathbf{H}_T \left(\mathbf{P}^-_{M|M} + \mathbf{Q}_T\right) \mathbf{H}_T^\top + \mathbf{R}_T \qquad (2) \\
\hat{\mathbf{z}}^+_{M|T} &= \hat{\mathbf{z}}^-_{M|M} + \mathbf{P}^- \mathbf{H}_T^\top \mathbf{\Sigma}^{-1}_{yy} (\tilde{\mathbf{y}}_T - \hat{\mathbf{y}}_T) \qquad (3) \\
\mathbf{P}^+_{M|T} &= \mathbf{P}^-_{M|M} - \mathbf{P}^-_{M|M} \mathbf{H}_T^\top \mathbf{\Sigma}^{-1}_{yy} \mathbf{H}_T \mathbf{P}^-_{M|M} \qquad (4)
\end{aligned}$$

This update to the previous MS state using TD information then primes $\hat{\mathbf{z}}^+_{M|T}$ and $\mathbf{P}^+_{M|T}$ to be used with a Kalman filter. Simple dynamics are used to propagate this state and covariance to the next MS

$$\begin{aligned}
\hat{\mathbf{z}}^+_{M|T} &\leftarrow \mathbf{D} \hat{\mathbf{z}}^+_{M|T} \qquad (5) \\
\mathbf{P}^+_{M|T} &\leftarrow \mathbf{D} \mathbf{P}^+_{M|T} \mathbf{D}^\top + \mathbf{Q}_M \qquad (6)
\end{aligned}$$

These simple dynamics change the signs of the lateral position and velocity of the CoM to emulate the switching of the stance foot and allow for the application of a standard Kalman filter from MS to MS. It is assumed that the motion of the CoM is periodic with respect to the stance foot; however, since the CoM position is referenced from the stance foot, which changes step to step, the lateral position and velocity also change signs. Therefore, the propagation matrix is $\mathbf{D} = \mathrm{diag}([1, -1, 1, 1, -1, 1, 1])$.

The second update takes place at the next MS, with the stance foot switched. The outputs of Eq. (5) and (6) are updated using a Kalman update

$$\begin{aligned}
\mathbf{K} &= \mathbf{P}^+_{M|T} \mathbf{H}_M^\top \left(\mathbf{H}_M \mathbf{P}^+_{M|T} \mathbf{H}_M^\top + \mathbf{R}_M\right)^{-1} \qquad (7) \\
\hat{\mathbf{z}}^+_{M|M} &= \hat{\mathbf{z}}^+_{M|T} + \mathbf{K}(\tilde{\mathbf{y}}_M - \mathbf{H}_M \hat{\mathbf{z}}^+_{M|T}) \qquad (8) \\
\mathbf{P}^+_{M|M} &= (\mathbf{I} - \mathbf{K}\mathbf{H}_M)\mathbf{P}^+_{M|T} \qquad (9)
\end{aligned}$$

where the measurement model Jacobian is $\mathbf{H}_M = \mathbf{I}^{6\times 7}$ since the measurements are $\tilde{\mathbf{y}}_M = [\tilde{\mathbf{p}}_{CoM}, \tilde{\mathbf{v}}_{CoM}]^\top$.

A conventional Kalman filter formulation applied to this problem would only take measurements at MS into account. However, the estimator setup presented in this work varies from that approach by taking information obtained at TD into account and updating the prior distribution for the Kalman filter. As the dynamics-free Bayesian update reinforces the MS-to-MS Kalman filter, this estimation setup has been termed as a Buttressed Kalman Filter.

The estimator needs to send an output signal to the exoskeleton to inform its controller of the user's intent. Since the representation of user intent was chosen to be the forward velocity, the change of $\hat{v}^d_x$ from MS to MS represents the user's desire to change gait speed. The estimator uses a simple model to predict the step length, so it does not emulate the exact relationship between the velocity at MS and the ensuing step length. As a result, using the estimated value of the intended velocity is not a good indicator of intent, as this value may not match the measured values. However, the change of the intended velocity from MS to MS Δv^d_x is a better candidate for intent change indication. This quantity represents the expected "acceleration" from MS to MS so it can be considered to be a "speed-up" signal when the rate is positive or a "slow-down" signal when the rate is negative. Inferring intent as a "speed-up" or "slow-down" signal is consistent with the fundamentally abstract nature of intent as opposed to the concrete velocity value given by the estimator. This ability to capture continuous adjustments may result in finer control of the exoskeleton compared to discrete activity classification that is more commonly used.

B. Utilizing Exoskeleton Data

The estimation framework outlined above was tested with data acquired during walking trials in an Ekso GT exoskeleton developed by Ekso Bionics. Sensors onboard the exoskeleton provide hip pitch, knee pitch, and torso roll angles, and are fused to estimate the height and fore-aft position of the hip in a global frame. These readings were used to approximate the location of the subject's CoM with respect to the stance foot. Since the position of the CoM is considered relative to the stance foot, the drift that may be present in the global position estimate does not affect step-to-step calculations. The subject's height, thigh, and shank lengths were recorded and the location of their CoM was approximated to be at the centroid of the pelvis. The remaining dimensions such as ankle height and hip width were computed using anthropometry relationships defined by Winter [30]. The CoM velocities were computed with finite-difference approximations.

The two main gait events to be identified for the estimator were MS and TD. A zero-crossing event between the left and right hip angles reported by the exoskeleton was used to detect MS. Force sensor readings from both feet being above a threshold of 5% of the maximum sensor value was indicative of touchdown. For healthy individuals walking independently, the foot touchdown process starts with a heel strike, the ankle then undergoes plantarflexion and the foot then rests flat on the ground. Plantarflexion is the motion of the foot about the ankle when it rotates away from the shank, and since the exoskeleton has no ankle mobility, the subject has to touch down with a nearly flat foot. This results in step lengths that are shorter than those observed in independent walking. Additionally, the subject walking in the exoskeleton used an ambulatory device such as a walker or crutches. Consequently, data from walking trials of subjects using the Ekso GT [31] was used in the regression for the step length model shown in Eq. (1). To perform the regression, the velocity at the subsequent MS was assumed to be the desired velocity. For example, suppose v_k was the forward velocity of the walker at MS at time k. The regression was set up such that $l_{step,k+1} = [v_k \ (v_{k+1} - v_k) \ l_{leg}]\boldsymbol{\kappa}$, where the subscript x has been omitted for conciseness, and the desired velocity was $v^d = v_{k+1}$. This formulation provided insight into the step length, using future velocity data to provide a proxy for the intended velocity.

III. Results & Discussion

A. Walking Trial Data Collection

Trial data was collected as part of a study approved by the IRB of the University of Notre Dame (Protocol 18-04-4650) [32]. Both, the exoskeleton users with and without injuries were highly experienced in the use of the EksoGT. The EksoGT has 4 motors, 2 revolute hip joints, and 2 revolute knee joints. All the motion takes place in the sagittal plane, the X-Z plane in Fig. 1. However, the lateral movement of the CoM is observed due to the roll angle of the torso relative to the vertical. The Ekso GT restricts torso roll with respect to the hips, such that the tilt angle of the pelvis in the frontal plane is the same as the torso roll. The subjects used the exoskeleton at a self-selected speed with the assistance of a walker and were at a steady-state gait before being issued a verbal command to either speed up or slow down. The trial sequence was pseudo-random and each subject underwent three speed-up (SU) and slow-down (SD) trials.

B. Subject without iSCI

The trial shown in this section was that of a subject without iSCI walking in free mode. In this mode, the exoskeleton provides constant assistance akin to gravity compensation to the user. The measurement used at TD was the step length, so the measurement vector was $\tilde{\mathbf{y}}_T = [l_{step}]$. Measurements of all positions and velocities were available at MS so $\tilde{\mathbf{y}}_M = [\mathbf{p}_{CoM}, \mathbf{v}_{CoM}]^\top$. The process noise covariance $\mathbf{Q}$ and the measurement noise covariance $\mathbf{R}$ were given by

$$\mathbf{Q}_M = \text{diag}([1,1,1,1,1,1,10]) \times 10^{-4} \quad (10)$$

$$\mathbf{R}_M = \text{diag}([10^4, 10^4, 10^4, 10^5, 1, 1]) \times 10^{-10} \quad (11)$$

$$\mathbf{Q}_T = 10^{-4} \quad (12)$$

$$\mathbf{R}_T = 10^{-5} \quad (13)$$

where process noise covariances for positions and velocities are reported with units m^2 and m^2/s^2 respectively.

The regression coefficients for the footstep model were $\boldsymbol{\kappa} = [0.3325, 0.2635, 0.3757]^\top$ for this subject. The step lengths for an SU trial are shown in Fig. 5. The regressed model was able to estimate the footstep to within $\sim$ 5cm with a RMS error of 2.5cm. Consequently, it will be observed that footstep changes alone provided sufficient information to estimate intent changes in this case. The data in Fig. 6 illustrates the estimator performance for this trial. The stem plot represents the intent of the user as inferred at TD; a positive value indicates speed-up and a negative value indicates slow-down anticipated for the subsequent MS. The vertical line represents the MS closest to the time the speed-change command was issued and a significant speed change is to be expected after this step. The estimator accurately estimated the speed change for the trials i.e., the value of the signal in the stem plot should be positive for speed-up and negative for slow-down after the command is issued.

The estimator performance for all trials of this subject are aggregated in Table. I. The "Command Step" column refers to the MS when the command was issued and the "Detection Step" refers to the step during which TD the intent change

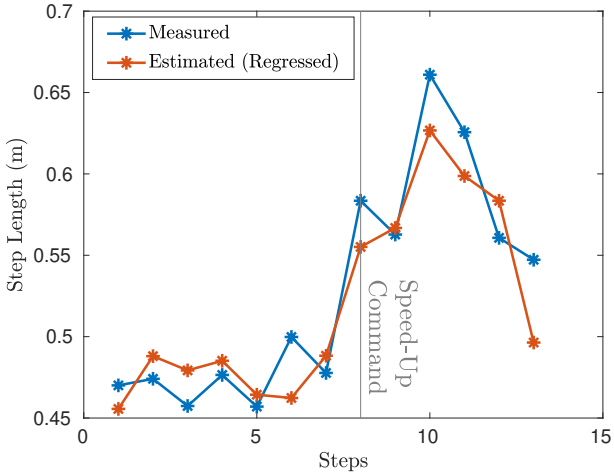

Fig. 5. Performance of the regressed model, Eq. (1), for the uninjured subject for a speed-up trial

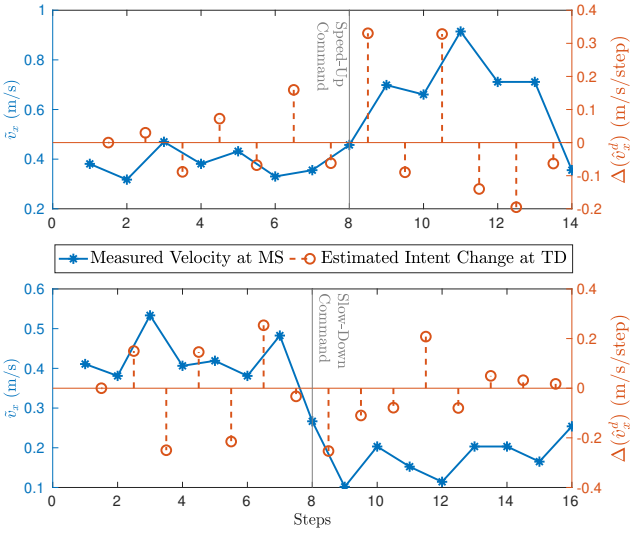

Fig. 6. Estimator performance for SU and SD trials for an uninjured subject

was detected. Since the user must first process the command given, an intent detection delay of up to one step was deemed permissible. All SU and SD trials fit this criteria.

For further analysis, the estimated change in v_x^d for every step was compared to the measured change. If the speed change sign was correctly anticipated, it was considered a successful trial. The probability of successful intent change inference for the aggregated trials of the uninjured subject was 69% with a 95% confidence interval [33] of 59% - 78%. The estimator has difficulty estimating intent changes when the velocity change is low, i.e., less than $\sim$ 0.15 m/s due to insufficient changes in step lengths. This may be the reason for a majority of the erroneous estimates.

C. Subject with iSCI

The subject whose trials were used for the following evaluation had previously experienced an incomplete SCI from

TABLE I
ESTIMATOR PERFORMANCE FOR TRIALS WITH AN UNINJURED SUBJECT

Trial	Command Step	Detection Step
SU - 01	8	8
SU - 02	8	8
SU - 03	8	9
SD - 01	7	7
SD - 02	7	7
SD - 03	7	7

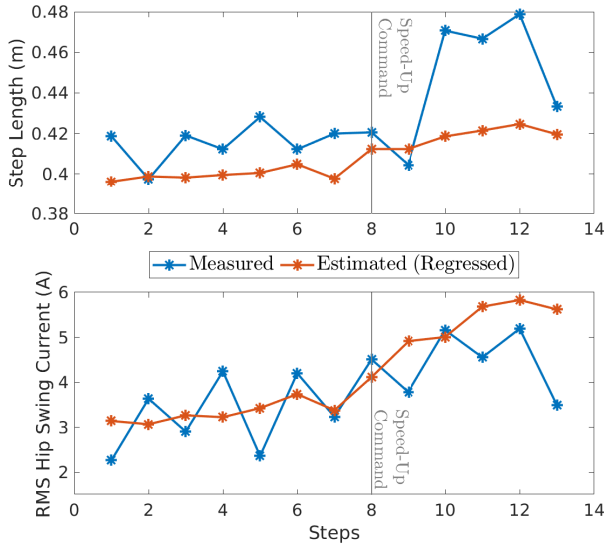

Fig. 7. Performance of the regressed models, Eqs. (1) and (14), for a subject with iSCI

the middle to the lower spine (T8 to L2). Individuals with these injuries generally exhibit good upper-body movement, control and balance but signals to the hips and legs are affected [34]. For use with such an injury, the exoskeleton was set to adaptive mode. In this mode, the exoskeleton joints follow predefined trajectories and correct any deviations from them. Consequently, intent change is perceived as a deviation from the preset trajectories and therefore the exoskeleton attempts to correct the user's gait.

The nature of the assistance provided in adaptive mode results in a difference in goals of the user and the robot after intent change. As a result, the step lengths did not exhibit significant enough variation or a consistent trend to allow for intent inference by themselves. The lack of step length variation is further supported by the regression coefficients for this subject $\boldsymbol{\kappa} = [0.0818, 0.0551, 0.4045]^\top$. When compared to the regression coefficients for the model for the uninjured user, the iSCI model regression coefficients for v_k and $(v_x^d - v_x)$ are smaller by an order of magnitude. This difference in coefficient magnitude shows there was not enough correlation between velocity changes and step length.

Figure 7 shows the step lengths for an SU trial; the estimated step lengths do not follow measurements, and only vary by $\sim$2 cm throughout the trial, whereas the measurements vary by $\sim$7 cm. Therefore, it was not possible to rely solely on footstep data. Thus, the RMS current of the hip motor during the swing

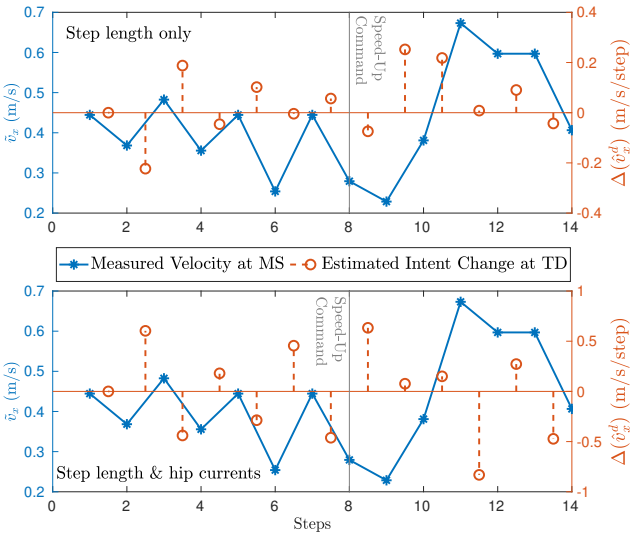

Fig. 8. Estimator performance comparison before and after including hip current measurements

phase was added to the measurements obtained at TD, so that $\tilde{\mathbf{y}}_T = [l_{step}, I_{RMS}]^\top$. Another regression was performed to establish a relationship between the intended velocities and swing current:

$$I_{RMS} = [v_x \ (v_x^d - v_x)]\boldsymbol{\alpha}, \tag{14}$$

where $\boldsymbol{\alpha}$ is a vector of the regression coefficients, found as $\boldsymbol{\alpha} = [8.6067, 4.2420]^\top$ for this trial.

The process noise covariance $\mathbf{Q}$ and the measurement noise covariance $\mathbf{R}$ were then selected as follows.

$$\mathbf{Q}_M = \text{diag}([1,1,1,1,1,1,10]) \times 10^{-4} \tag{15}$$
$$\mathbf{R}_M = \text{diag}([10^4, 10^4, 10^4, 10^5, 1, 1]) \times 10^{-10} \tag{16}$$
$$\mathbf{Q}_T = 10^{-3} \tag{17}$$
$$\mathbf{R}_T = \text{diag}([1,1]) \times 10^{-4} \tag{18}$$

where noise covariances for positions, velocities, and currents are reported with units m^2, m^2/s^2, and A^2 respectively.

The hip current, in addition to the footstep data, provided sufficient information to be able to infer the user's intent immediately after the speed-change command was issued. The performance of estimator for one of the SU trials with and without hip current measurements is illustrated in Fig. 8. When relying solely on step length measurements, the estimator was unable to output accurate speed-up/slow-down signals in the beginning of the trial, and the change in intent to speed up was detected a step after the command was issued. There was a small dip of 0.05 m/s in velocity after the speed up command was issued and this may be because the exoskeleton assistance in adaptive mode overpowered the user's motion in order to maintain the nominal joint trajectory. However, with the inclusion of hip motor currents, the estimator was able to correctly identify the change in intent to speed up during the same step the command was issued and before the user began physically speeding up. This anticipative performance of the estimator is shown in Fig. 9 for additional SU and SD trails.

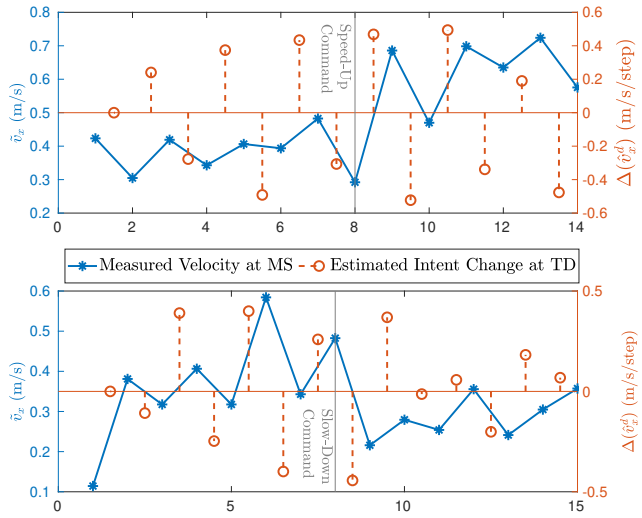

Fig. 9. Estimator performance for SU and SD trials for a subject with iSCI

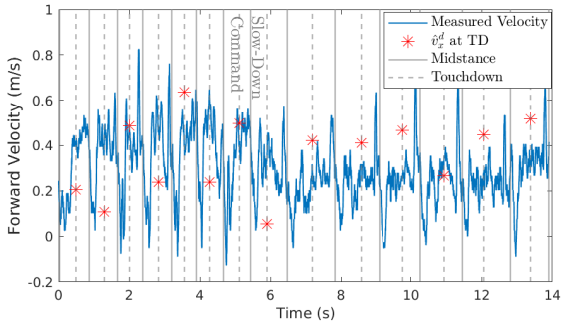

Fig. 10. Estimated desired velocity at MS as predicted at TD ($\hat{v}_x^d$) compared to velocity v_x over the stride.

The estimated value of $\hat{v}_x^d$ for one SU trial was compared to the measured forward velocity over the trial, as illustrated in Fig. 10. The vertical solid lines denote MS, dashed lines denote TD, and red stars denote the value of $\hat{v}_x^d$, i.e., the estimate of the user's intended velocity. Since $\hat{v}_d^x$ represents the desired speed of the user, its value at TD was compared to the measured velocity at the subsequent MS, by which point the intended velocity should be realized. The values of $\hat{v}_x^d$ predicted at TD show strong correlation with the measured values of v_x at the next MS, but are not exact. For the trial illustrated in Fig. 10, the correlation coefficient of $\hat{v}_x^d$ at TD to the measured v_x at the next MS was 0.63. By comparison, the correlation coefficient of $\hat{v}_x$ at TD to the measured v_x at the next MS was -0.11. This correlation further bolsters the hypothesis that incorporating information at touchdown in the estimator is valuable for anticipating speed changes.

The estimator performance for all trials of this subject is aggregated in Table II with similar pass/fail criteria as the trials with the uninjured subject. For trial SD-03, the estimator detected the speed change after the command but there were estimator inaccuracies for the subsequent step. There were

TABLE II
ESTIMATOR PERFORMANCE FOR TRIALS WITH A SUBJECT WITH AN ISCI

Trial	Command Step	Detection Step
SU - 01	8	8
SU - 02	8	8
SU - 03	7	11
SD - 01	8	8
SD - 02	7	7
SD - 03	8	8

fluctuations of ∼0.15 m/s in the forward velocity of the user after the command was issued. This may be due to the high gait variability due to spastic disturbances that are common in individuals with SCIs [35]. It has been observed that it is more difficult to detect speed-up intent changes in injured individuals since the intent signal is considerably diminished compared to slow-down trials [32] due to the user's reduced strength.

The aggregate probability of success for walking trials of the subject with iSCIs was 78% with a 95% confidence interval of 68% to 86%. All trials except SD-03 had individual percentages of success of at least 70%. Trial SU-02 had a probability of success of 92% and SU-01 and SD-01 had a 100% success rate. It is worth noting that the trials with high success rates were performed when the subject was rested and SD-03 was the last of multiple back-to-back trials. The subject's exhaustion may have diminished their ability to resist the exoskeleton's inputs and therefore, made intent estimation difficult.

IV. CONCLUSION & FUTURE WORK

In conclusion, the intent detection framework based on a Buttressed Kalman Filter is capable of predicting intent changes in both able-bodied and non able-bodied exoskeleton users based on foot placement and leg swing currents. It can be inferred that the hip currents may be a better indicator of intent in individuals with iSCIs as their actions to modify their foot placement may not be completed due to the resistance from the exoskeleton. So we can argue that attempted foot placement is the primary mechanism of exhibiting intent change in individuals with iSCIs, but the human-robot interface causes this information to show up on hip current rather than kinematic data.

The accuracy of the estimator can be further increased by improving the models used to relate velocity changes to the measured step length and current. These models may change based on the user and the ambulatory device used in conjunction with the exoskeleton. The estimator uses simple dynamics that do not use knowledge of legged locomotion. These simple dynamics along with the limited data to generate the footstep model result in the framework only being able to identify whether the user wants to speed up or slow down and not the target velocity the user wishes to reach. The behavior may be remedied by using a more descriptive foot placement model that establishes a more precise relationship between intended gait velocity and foot placement. Due to the difficulty in identifying the threshold for the intent signal, it is difficult to gauge the magnitude of the necessary intent change. Improving

the measurement models may yield a more accurate estimate of the intended gait speed, which may help transition the intent detection to a form with more resolution than speed-up or slow-down. Additionally, the applicability of models to users outside the training dataset also needs to be investigated in order to be able to accommodate a larger number of users.

The presented intent change detection framework updates the intent change estimate once per step. To improve the robustness against misclassification, future work may consider fusing this strategy with other intent change estimators (e.g., [21]) that draw upon other sources of information across the gait cycle. The walking trials display the inability of the user with iSCI to resist the exoskeleton's trajectory tracking to carry out intent changes. These difficulties highlight the importance of the intent detection advances herein to improve the robot's ability to anticipate the user's actions and increase HRI fluidity.

REFERENCES

[1] "Spinal cord injury: Hope through research." [Online]. Available: https://www.ninds.nih.gov/Disorders/Patient-Caregiver-Education/Hope-Through-Research/Spinal-Cord-Injury-Hope-Through-Research

[2] L. Brenner, "Exploring the psychosocial impact of ekso bionics technology," *Archives of Physical Medicine and Rehabilitation*, vol. 97, no. 10, p. e113, 2016.

[3] "Rewalk personal exoskeleton system cleared by FDA for home use," https://rewalk.com/rewalk-robotics-announces-expansion-to-india-with-saimed-innovations-2-2-2-2-3-2-3/.

[4] F. Sup, A. Bohara, and M. Goldfarb, "Design and control of a powered transfemoral prosthesis," *The International Journal of Robotics Research*, vol. 27, no. 2, pp. 263–273, 2008.

[5] J. Hidler and R. Sainburg, "Role of robotics in neurorehabilitation," *Topics in Spinal Cord Injury Rehabilitation*, vol. 17, no. 1, pp. 42–49, 2011.

[6] G. Hoffman and C. Breazeal, "Cost-based anticipatory action selection for human–robot fluency," *IEEE Transactions on Robotics*, vol. 23, no. 5, pp. 952–961, 2007.

[7] J. W. Crandall, M. A. Goodrich, D. R. Olsen, and C. W. Nielsen, "Validating human-robot interaction schemes in multitasking environments," *IEEE Transactions on Systems, Man, and Cybernetics-Part A: Systems and Humans*, vol. 35, no. 4, pp. 438–449, 2005.

[8] B. Shen, J. Li, F. Bai, and C.-M. Chew, "Motion intent recognition for control of a lower extremity assistive device (lead)," in *IEEE International Conference on Mechatronics and Automation*, 2013, pp. 926–931.

[9] B. Corteville, E. Aertbeliën, H. Bruyninckx, J. De Schutter, and H. Van Brussel, "Human-inspired robot assistant for fast point-to-point movements," in *IEEE International Conference on Robotics and Automation*, 2007, pp. 3639–3644.

[10] A. U. Pehlivan, D. P. Losey, and M. K. O'Malley, "Minimal assist-as-needed controller for upper limb robotic rehabilitation," *IEEE Transactions on Robotics*, vol. 32, no. 1, pp. 113–124, 2015.

[11] D. Brescianini, J.-Y. Jung, I.-H. Jang, H. S. Park, and R. Riener, "INS/EKF-based stride length, height and direction intent detection for walking assistance robots," in *IEEE International Conference on Rehabilitation Robotics*, 2011, pp. 1–5.

[12] K. Suzuki, G. Mito, H. Kawamoto, Y. Hasegawa, and Y. Sankai, "Intention-based walking support for paraplegia patients with robot suit HAL," *Advanced Robotics*, vol. 21, no. 12, pp. 1441–1469, 2007.

[13] H. Geyer, A. Seyfarth, and R. Blickhan, "Compliant leg behaviour explains basic dynamics of walking and running," *Proceedings of the Royal Society B: Biological Sciences*, vol. 273, no. 1603, pp. 2861–2867, 2006.

[14] Y. Liu, P. M. Wensing, D. E. Orin, and Y. F. Zheng, "Dynamic walking in a humanoid robot based on a 3D actuated Dual-SLIP model," in *IEEE International Conference on Robotics and Automation*, 2015, pp. 5710–5717.

[15] R. M. Karulkar and P. M. Wensing, "Application of interacting models to estimate the gait speed of an exoskeleton user," in *IEEE International Conference on Intelligent Robots and Systems*, 2020.

[16] J. R. Nymark, S. J. Balmer, E. H. Melis, E. D. Lemaire, and S. Millar, "Electromyographic and kinematic nondisabled gait differences at extremely slow overground and treadmill walking speeds." *Journal of Rehabilitation Research & Development*, vol. 42, no. 4, 2005.

[17] A. D. Kuo, "A simple model of bipedal walking predicts the preferred speed–step length relationship," *Journal of Biomechanical Engineering*, vol. 123, no. 3, pp. 264–269, 2001.

[18] U. H. Lee, J. Bi, R. Patel, D. Fouhey, and E. Rouse, "Image transformation and cnns: A strategy for encoding human locomotor intent for autonomous wearable robots," *IEEE Robotics and Automation Letters*, vol. 5, no. 4, pp. 5440–5447, 2020.

[19] N. Thatte, T. Shah, and H. Geyer, "Robust and adaptive lower limb prosthesis stance control via extended kalman filter-based gait phase estimation," *IEEE Robotics and Automation Letters*, vol. 4, no. 4, pp. 3129–3136, 2019.

[20] A. Kalinowska, T. A. Berrueta, A. Zoss, and T. Murphey, "Data-driven gait segmentation for walking assistance in a lower-limb assistive device," in *IEEE International Conference on Robotics and Automation*, 2019, pp. 1390–1396.

[21] T. Gambon, J. P. Schmiedeler, and P. M. Wensing, "User intent identification in a lower-extremity exoskeleton via the mahalanobis distance," in *IEEE RAS/EMBS International Conference on Biomedical Robotics and Biomechatronics*, 2020, pp. 1115–1121.

[22] A. L. Hof, S. Vermerris, and W. Gjaltema, "Balance responses to lateral perturbations in human treadmill walking," *Journal of Experimental Biology*, vol. 213, no. 15, pp. 2655–2664, 2010.

[23] J. Dingwell, J. Cusumano, P. Cavanagh, and D. Sternad, "Local dynamic stability versus kinematic variability of continuous overground and treadmill walking," *J. Biomech. Eng.*, vol. 123, no. 1, pp. 27–32, 2001.

[24] Y. Wang and M. Srinivasan, "Stepping in the direction of the fall: the next foot placement can be predicted from current upper body state in steady-state walking," *Biology letters*, vol. 10, no. 9, p. 20140405, 2014.

[25] N. Sekiya, H. Nagasaki, H. Ito, and T. Furuna, "Optimal walking in terms of variability in step length," *Journal of Orthopaedic & Sports Physical Therapy*, vol. 26, no. 5, pp. 266–272, 1997.

[26] B. Bogen, R. Moe-Nilssen, A. H. Ranhoff, and M. K. Aaslund, "The walk ratio: Investigation of invariance across walking conditions and gender in community-dwelling older people," *Gait & posture*, vol. 61, pp. 479–482, 2018.

[27] R. Murakami and Y. Otaka, "Estimated lower speed boundary at which the walk ratio constancy is broken in healthy adults," *Journal of physical therapy science*, vol. 29, no. 4, pp. 722–725, 2017.

[28] V. Rota, L. Perucca, A. Simone, and L. Tesio, "Walk ratio (step length/cadence) as a summary index of neuromotor control of gait: application to multiple sclerosis," *International journal of rehabilitation research*, vol. 34, no. 3, pp. 265–269, 2011.

[29] K. Seo, S. Hyung, B. K. Choi, Y. Lee, and Y. Shim, "A new adaptive frequency oscillator for gait assistance," in *IEEE International Conference on Robotics and Automation*, 2015, pp. 5565–5571.

[30] D. A. Winter, *Biomechanics and motor control of human movement*. John Wiley & Sons, 2009.

[31] T. Gambon, "Onboard exoskeleton data during user intent changes," 2020. [Online]. Available: https://dx.doi.org/10.21227/r9ap-mk26

[32] T. M. Gambon, J. P. Schmiedeler, and P. M. Wensing, "Effects of user intent changes on onboard sensor measurements during exoskeleton-assisted walking," *IEEE Access*, 2020.

[33] L. D. Brown, T. T. Cai, and A. DasGupta, "Interval estimation for a binomial proportion," *Statistical science*, pp. 101–117, 2001.

[34] "Spinal cord injury." [Online]. Available: https://www.christopherreeve.org/living-with-paralysis/health/causes-of-paralysis/spinal-cord-injury

[35] S. Malhotra, A. Pandyan, C. Day, P. Jones, and H. Hermens, "Spasticity, an impairment that is poorly defined and poorly measured," *Clinical rehabilitation*, vol. 23, no. 7, pp. 651–658, 2009.